REGULAR ARTICLES

Food chain chaos due to Shilnikov's orbit

Bo Deng[a] and Gwendolen Hines[b]
Department of Mathematics and Statistics, University of Nebraska–Lincoln, Lincoln, Nebraska 68588

(Received 11 January 2002; accepted 8 April 2002; published 3 June 2002)

Assume that the reproduction rate ratio ζ of the predator over the prey is sufficiently small in a basic tri-trophic food chain model. This assumption translates the model into a singularly perturbed system of two time scales. It is demonstrated, as a sequel to the earlier paper of Deng [Chaos **11**, 514–525 (2001)], that at the singular limit $\zeta=0$, a singular Shilnikov's saddle-focus homoclinic orbit can exist as the reproduction rate ratio ε of the top-predator over the predator is greater than a modest value ε_0. The additional conditions under which such a singular orbit may occur are also explicitly given. © *2002 American Institute of Physics.* [DOI: 10.1063/1.1482255]

Ecocomplexity may not be properly understood without understanding the role chaos plays in food chains. Yet chaos generating mechanisms have not been systematically categorized in the literature. The purpose of this paper is to continue the chaos classification program initiated in Ref. 1 and to add a second chaos generation mechanism to the list.

I. INTRODUCTION

The seminal work of Lotka[2] and Volterra[3] laid the foundation of mathematical modeling for population dynamics. The logistic model has been accepted by modelers for species dynamics free of predation but constrained to resource-limited habitats. Holloing's seminal work[4] on predation functional forms provided the biological bases for predator–prey and n-trophic Rosenzweig–MacArthur models[5] for food chains. Plausible population models in continuous times from literature are mostly variations of the Rosenzweig–MacArthur models.

Because of their perceived intrinsic relevance to biology, these models have generated an enormous amount of research and continue to attract more people to an ever-expanding field, not just because there are too numerous types of species interactions to consider, but also because even the simplest basic tri-trophic models pose some extremely challenging mathematical problems. Above all, chaos is least understood for these models, at least from the point of view of mathematics—there was not a single theorem obtained on the existence of any food chain model chaos prior to Ref. 1. In contrast a tremendous amount of rigorous results have been published on equilibrium and periodic solutions, see, e.g., Refs. 6–8. This void in theoretical food chain chaos is more considerable given the fact that the first food chain chaos models were discovered almost a quarter century ago in Refs. 9 and 10.

Although chaotic structures were continuously discovered, e.g., Refs. 11, 8, 12–16, from numerous food chain models, systematic approaches to classification were hampered by a lack of effective handles on the models. First, studies are scattered among models as diversified as biology. Second, there was not a single dimensionless form, which always constitutes the first step in any mathematical study, that was used by any competing research groups, rarely used twice within a group, or by an individual. Multi-time scale approach was first used in Ref. 7 for food chain models, but the lack of a proper transformation that could bring the multi-time scaled model of Ref. 7 to bear prevented this approach from taking its hold, at least until the scaling of Ref. 1. Numerical mapping of bifurcation diagrams, two parameters at a time, were carried out in Refs. 15 and 16 thanks to the advent of computer computing as a brute force but powerful tool. Results of this kind, however, are mostly observational and narrative by nature.

Types of food chain model chaos were limited to the Rössler type[17] of earlier findings,[9,10,18] expanded to the teacup type of Ref. 11, and the Shilnikov type[19] of Ref. 12. Classification was mostly based on visual inspection. Mechanistic identification for Shilnikov's saddle-focus homoclinic orbits was carried out numerically in Ref. 15. The purpose of this paper is to continue the mechanistic approach via the multi-time scale analysis adopted in Ref. 1 and to find system parameter conditions by which the Shilnikov chaos scenario can take place in the Rosenzweig–MacArthur model. The parameter region applies to food chains of which, in terms of allometry,[20,21] the biomass of the prey is small relative to that of the predator, which in turn is comparable with the biomass of the top-predator.

II. PRELIMINARY ANALYSIS

We continue to consider the following Rosenzweig–MacArthur model[5] for food chains analyzed in Ref. 1:

[a]Electronic mail: bdeng@math.unl.edu
[b]Electronic mail: ghines@math.unl.edu

$$\dot{x}=x\left(r-\frac{rx}{K}-\frac{p_1y}{H_1+x}\right),$$

$$\dot{y}=y\left(\frac{c_1x}{H_1+x}-d_1-\frac{p_2z}{H_2+y}\right), \tag{2.1}$$

$$\dot{z}=z\left(\frac{c_2y}{H_2+y}-d_2\right),$$

with a logistic prey (x), a Holloing type II predator (y), and a Holling type II top-predator (z).[4] With the same scaling of variables and parameters as in Ref. 1,

$$t\to c_1t,\quad x\to\frac{1}{K}x,\quad y\to\frac{p_1}{rK}y,\quad z\to\frac{p_2p_1}{c_1rK}z,$$

$$\zeta=\frac{c_1}{r},\quad \varepsilon=\frac{c_2}{c_1},\quad \beta_1=\frac{H_1}{K},\quad \beta_2=\frac{H_2}{Y_0} \tag{2.2}$$

with

$$Y_0=\frac{rK}{p_1},\quad \delta_1=\frac{d_1}{c_1},\quad \delta_2=\frac{d_2}{c_2},$$

Eq. (2.1) is changed to the following dimensionless form:

$$\zeta\dot{x}=x\left(1-x-\frac{y}{\beta_1+x}\right):=xf(x,y),$$

$$\dot{y}=y\left(\frac{x}{\beta_1+x}-\delta_1-\frac{z}{\beta_2+y}\right):=yg(x,y,z), \tag{2.3}$$

$$\dot{z}=\varepsilon z\left(\frac{y}{\beta_2+y}-\delta_2\right):=\varepsilon zh(y).$$

Under the drastic trophic time diversification hypothesis[1] that *the maximum per-capita growth rate decreases from bottom to top along the food chain*, namely

$$r\gg c_1\gg c_2>0 \text{ or equivalently } 0<\zeta\ll 1 \text{ and } 0<\varepsilon\ll 1,$$

Eqs. (2.3) become a singularly perturbed system of three time scales, with the rates of change for the prey, predator, and top-predator ranging from fast to intermediate to slow, respectively. Let $\bar{y}$ be the maximum of the nontrivial x-nullcline $\{f(x,y)=0\}$ and $y_{\rm spk}$ be the point of Pontryagin's delay of stability loss[22–25,1] determined from the integral

$$\int_{y_{\rm spk}}^{\bar{y}}\frac{f(0,\xi)}{\xi g(0,\xi,z)}d\xi=0. \tag{2.4}$$

Then Ref. 1 shows that a period-doubling cascade reversal must occur as the nontrivial z-nullcline $h(y)=0$ crosses the surface of Pontryagin's delay of stability loss $y=y_{\rm spk}(z)$ from below due to the occurrence of junction-fold points at which solutions of the equations have a quadratic-like tangency with the plane $y=y_{\rm spk}(z)$.

In this paper, we assume the time diversification hypothesis for the prey–predator interaction only:

$$r\gg c_1>0 \text{ or equivalently } 0<\zeta\ll 1, \tag{2.5}$$

and leave the rate between c_1 and c_2 comparable, which applies to cases where the body masses of the predator and the top-predator are comparable according to the theory of allometry.[20,21] Under this assumption, Eq. (2.3) is a two-time-scale singularly perturbed system whose dynamics are most determined by the predator–top-predator interactions on the trivial x-nullcline $x=0$ and the attracting part of the nontrivial x-nullcline parabola $\{f(x,y)=0\}$ which contains the nontrivial equilibrium point $p_f=(x_f,y_f,z_f)$. We will demonstrate that the equilibrium point p_f becomes a saddle focus as ε is greater than some value ε_0 and that under appropriate conditions there is a singular homoclinic orbit[26] to p_f at $\zeta=0$. Chaotic dynamics ensues both at the singular limit $\zeta=0$ by the result of Ref. 26 and with perturbation $0<\zeta\ll 1$ due to the conjectured existence of a persisting Shilnikov's saddle-focus homoclinic orbit.[19,27]

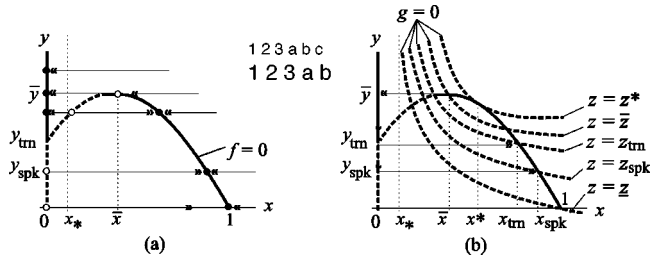

FIG. 1. (a) Phase lines and the x-nullcline surfaces $x=0$ and $f=0$ for the fast subsystem. Points of $x=0$, $y_{\rm trn}<y$ and $f(x,y)=0$, $\bar{x}<x$ are the only stable equilibrium points. (b) y-nullclines on various z sections giving a geometric illustration to the corresponding expressions in z.

III. SINGULAR PERTURBATION

The dimensionless system (2.3) with one singular parameter $0<\zeta\ll 1$ makes it ideal for a singular perturbation analysis.[7,28,29,26] The key is to reduce the dimension of the system from three to two or one using two different time scales and to piece together the lower dimensional structures to construct a full picture of the three-dimensional system.

A. The fast prey dynamics

By rescaling the time $t\to t/\zeta$ for Eq. (2.3) and setting $\zeta=0$, the rescaled system becomes

$$x'=xf(x,y),\quad y'=0,\quad z'=0.$$

It is one-dimensional in x variable with y and z as parameters. The flow of this so-called fast subsystem is completely determined by its equilibrium surface $xf(x,y)=0$, which is composed of $x=0$ and $f(x,y)=0$, in particular, by the stable equilibrium points. The surface $f(x,y)=0$ is a cylindrical parabola

$$y=(1-x)(\beta_1+x).$$

It has its maximum point and maximum value as

$$\bar{x}=\frac{1-\beta_1}{2},\quad \bar{y}=\frac{(1+\beta_1)^2}{4}.$$

It intersects the trivial equilibrium surface $x=0$ at

$$y=y_{\rm trn}=\beta_1.$$

See Figs. 1 and 2. Of the x-nullcline surfaces only two branches are attracting, which are $\{x=0,y>\beta_1\}$ and $\{f=0,x>\bar{x}\}$. When the system is in a perturbed state with 0

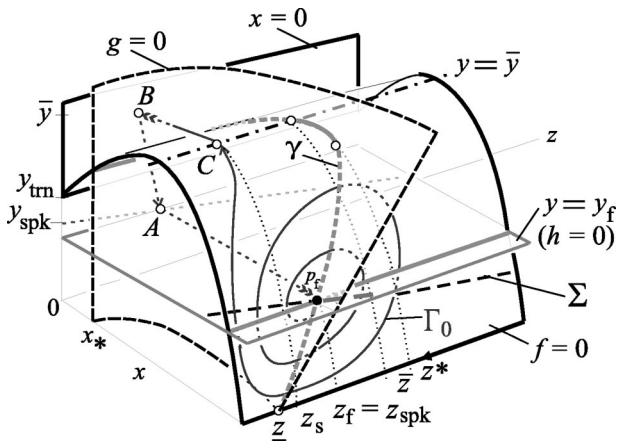

FIG. 2. Nullcline surfaces drawn in the full three-dimensional phase space. The jump from the fold $y=\overline{y}$, $x=\overline{x}$ to the x-stable part of the manifold $x=0$ in the direction of x is fast, so is the jump from $y=y_{\rm spk}$ to Σ. The crawl on the x-stable part of the parabola $f=0$ in y and z is slow compared to the x-fast jump. $\Gamma_0=p_fCBAp_f$ is a singular homoclinic orbit.

$<\zeta\ll 1$, all solutions are quickly attracted to either $\{x=0, y>\beta_1\}$ or $\{f=0, x>\overline{x}\}$ because the rate of change for x is much greater than those of y and z if the starting point is not near either of these two surfaces.

B. The slow predator and top-predator dynamics

When a solution for the perturbed system with $0<\zeta\ll 1$ is attracted near one of the two surfaces $\{x=0, y>\beta_1\}$ and $\{f=0, x>\overline{x}\}$, the solution is approximated by the reduced slow dynamics on either of the surfaces by setting $\zeta=0$ in Eq. (2.3)

$$xf(x,y)=0, \quad \dot{y}=yg(x,y,z), \quad \dot{z}=\varepsilon z h(y).$$

It is a two-dimensional system in y,z restricted on either $x=0$ or $\{f(x,y)=0\}$.

On the trivial surface $x=0$,

$$\dot{y}=yg(0,y,z)=y\left(-\delta_1-\frac{1}{\beta_2+y}z\right)<0,$$

$$\dot{z}=\varepsilon z h(y)=\varepsilon z\left(\frac{y}{\beta_2+y}-\delta_2\right).$$

Because $\dot{y}<0$, all solutions develop downward, attracted to $y=0$. It must cross the transcritical point $y_{\rm trn}=\beta_1$ at which the two branches of the x-nullcline intersect: $\{x=0\}\cap\{f(x,y)=0\}$. Once that point is passed, the lower, trivial branch $\{x=0, y<y_{\rm trn}\}$ is not attracting anymore. Solutions nearby are repelled away toward the stable branch $\{f(x,y)=0, x\geqslant\overline{x}\}$. By the theory of *Pontryagin's delay of stability loss*,[22–25] the reduced solutions on $x=0$ approximate the perturbed ones only to a point $y_{\rm spk}<y_{\rm trn}=\beta_1$, referred to as the point of *Pontryagin's delay of stability loss*. The point $y_{\rm spk}$ depends on where the perturbed solution starts. For example, if it starts with the initial y at $\overline{y}$, then $y_{\rm spk}$ is determined by the integral equation (2.4). If it starts at any other initial point in y, then $y_{\rm spk}$ is determined by the same integral with $\overline{y}$ replaced by that initial y. It is proved in Ref. 24 that $y_{\rm spk}$ defined by Eq. (2.4) is a monotone decreasing function in z. The $y_{\rm spk}$ depicted in Fig. 2 and throughout from now on is with the initial $\overline{y}$ value as in the integral equation (2.4) and Σ is its horizontally projected point on the x-attracting surface $\{f(x,y)=0, x>\overline{x}\}$.

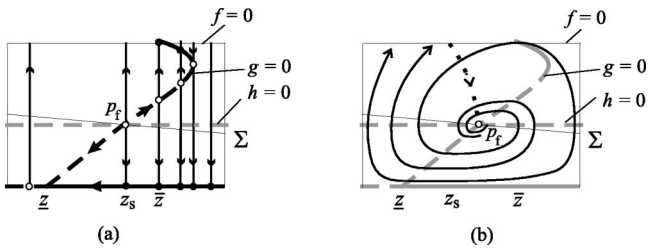

FIG. 3. Slow dynamics. (a) $\varepsilon=0$. (b) $\varepsilon>\varepsilon_0=a/4bm$. The dotted curve is the slow flow segment BA from the trivial x-nullcline.

On the nontrivial, stable x-nullcline surface $\{f(x,y)=0, x>\overline{x}\}$, the slow dynamics in (y,z) is more complex but two-dimensional nonetheless. Because it is two-dimensional, a phase plane analysis is utilized. The dynamics is determined by the y-nullcline $\{y=0\}$, $\{g(x,y,z)=0\}$ and the z-nullcline $\{z=0\}$, $\{h(y)=0\}$. Two of which, $\{y=0\}$ and $\{z=0\}$, are invariant and the dynamics on them are simple one-dimensional. The other two play the essential role. Denote the nontrivial y-nullcline on $\{f(x,y)=0, x>\overline{x}\}$ by $\gamma=\{g(x,y,z)=0\}\cap\{f(x,y)=0, x>\overline{x}\}$ as shown in Fig. 2. The nontrivial z-nullcline $h(y)=0$ is solved as $y=y_f=\beta_2\delta_2/(1-\delta_2)$. If we look at the three-dimensional illustration Fig. 2 in the direction of the x axis, then Fig. 3 is what it looks like: a projected view to the yz plane.

Conditions on parameters β_1,δ_1,β_2 were given in Proposition 6.5 of Ref. 1 that give rise to the exact depiction of the y-nullcline γ as in Figs. 2 and 3. In particular the condition

$$\underline{z}<z_{\rm spk}<\overline{z} \tag{3.1}$$

holds. Notice that because the parameter δ_2 is free from the above-mentioned condition, it can be changed so that $y_{\rm spk}=y_f=\beta_2\delta_2/(1-\delta_2)$. That is, when

$$\delta_2=y_{\rm spk}/(\beta_2+y_{\rm spk}), \tag{3.2}$$

the equilibrium point p_f falls on the Pontryagin landing curve Σ. This fact will be used later.

IV. SADDLE-FOCUS EQUILIBRIUM

In this section we consider in greater detail the reduced slow yz dynamics on the attracting x-nullcline surface $\{f(x,y)=0, x>\overline{x}\}$ and demonstrate that there exists a constant $\varepsilon_0>0$ such that the equilibrium point p_f becomes a saddle-focus for the reduced system when $\varepsilon>\varepsilon_0$.

Figure 3(a) shows the reduced phase portrait case when $\varepsilon=0$, in which case the slow dynamics is reduced to one-dimensional flow in y parametrized by z and the vertical phase lines are as shown. In particular, the eigenvalue, λ_1, of the linearized vector field at the equilibrium point that corresponds to the y dynamics is positive and that corresponds to the z dynamics, λ_2, is zero. For $\varepsilon>0$, $\dot{z}>0$ for points above the z-nullcline $y=y_f$, and $\dot{z}<0$ for points below it. Therefore the equilibrium point p_f is an unstable source as shown.

That is, the second eigenvalue $\lambda_2>0$ becomes positive for small positive $\varepsilon>0$, satisfying $\lambda_2=0$ as $\varepsilon=0$. As a result, the reduced vector field has a tendency to rotate around the equilibrium point p_f. Intuitively, the greater $\varepsilon>0$ is, the more pronounced the rotation becomes, and when ε is sufficiently away from 0, the eigenvalues λ_1,λ_2 become a pair of complex conjugates with positive real part. When that happens, p is an unstable focus.

What is described above can be stated in a more general manner. More specifically, the linearized vector field of the reduced subsystem must have the following form

$$\dot{y}=a[(y-y_f)-m(z-z_f)], \quad \dot{z}=\varepsilon b(y-y_f), \tag{4.1}$$

with positive constants a,b,m. In fact, the linearized y-nullcline $(y-y_f)=m(z-z_f)$ is precisely the tangent line to the original y-nullcline γ at p_f and $\dot{y}>0$ if and only if the point is above the y-nullcline. Similarly, the linearized z-nullcline $y=y_f$ is the same as the original horizontal z-nullcline and $\dot{z}>0$ if and only if the point is above the z-nullcline. a,b are parameter-dependent expressions resulting from the actual linearization. Parameter ε is preserved in the same position as a constant multiple to the original z equation. With the general form of the linearization in place, we can find its characteristic equation as $\lambda^2-a\lambda+\varepsilon abm=0$ and the eigenvalues are

$$\lambda_{1,2}=\frac{a\pm\sqrt{a^2-4\varepsilon abm}}{2}.$$

They becomes a pair of complex conjugates when $a^2-4\varepsilon abm<0$, or equivalently, when

$$\varepsilon>\varepsilon_0:=\frac{a}{4bm}. \tag{4.2}$$

And the equilibrium point p_f becomes an unstable focus on $\{f(x,y)=0,x>\overline{x}\}$.

V. SINGULAR HOMOCLINIC ORBIT

Under the conditions of Eqs. (3.1), (3.2), (4.2), and $\zeta=0$, there must exist a singular homoclinic orbit, Γ_0, to *either* p_f as shown in Fig. 2, *or* an unstable limit cycle surrounding p_f on the parabola x-nullcline surface $\{f=0,\overline{x}\leqslant x\leqslant 1\}$.

More precisely, directly opposite to p_f is a point A in the Pontryagin jumping curve $y=y_{\rm spk}$ in $\{x=0\}$ from which the fast x flow jumps from A to p_f. Going backward in the reduced yz flow on $\{x=0\}$, there is a point B on the line $y=\overline{y}$ from which the slow yz flow connects to A. Similarly, opposite to B is a point C on the turning point line $\{y=\overline{y},x=\overline{x}\}$ from which the fast x flow connects to B. Let z_s be the z coordinate of the point C. Then for $\varepsilon=0,z_s=z_{\rm spk}<\overline{z}$, and for $\varepsilon>0,z_s<z_{\rm spk}<\overline{z}$ as shown in Figs. 3(a) and 3(b). The reason that $z_s<z_{\rm spk}$ with $\varepsilon>0$ is because the slow segment AB lies mostly above the z-nullcline and it flows rightwards from B to A. Now since C lies left of the y-nullcline γ for $z_s<\overline{z}$, it is connected backward in asymptotic time either to the unstable spiral source p_f or an unstable periodic cycle on the parabola x-nullcline surface $\{f=0,\overline{x}\leqslant x\leqslant 1\}$ that encloses p_f. Without such a cycle, the existence of the singular homoclinic orbit $\Gamma_0=p_fCBAp_f$ is established, as shown in Figs. 2 and 3(b). If there is an unstable limit cycle, it must encircle the equilibrium point p_f by the Poincaré–Bendixson theorem. Thus the cycle must intersect the junction curve Σ at two points. Substituting the left intercept of the outermost cycle for p_f in the entire above-presented argument results in the second alternative statement that there exists a singular homoclinic orbit to a periodic orbit. In such a case chaos must occur according to the scenario of Ref. 30. Therefore, we have proven the following result.

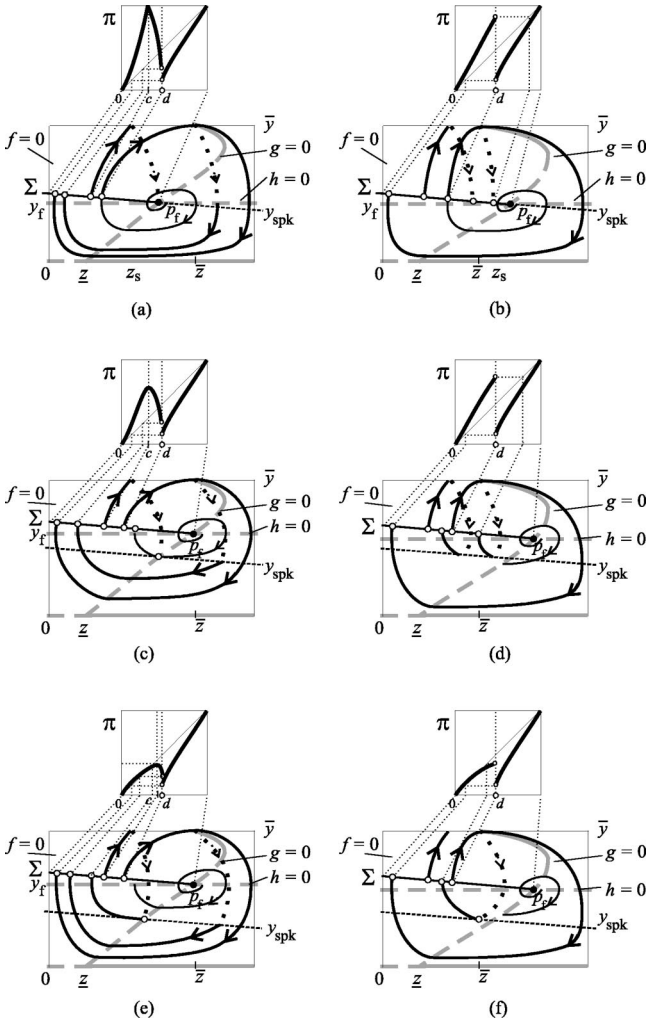

FIG. 4. Singular return maps π and their bifurcations. Dotted arrow curves are reduced slow yz flows on the trivial x-nullcline $x=0$.

Theorem 5.1: *Under the conditions of (3.1), (3.2), (4.2), and* $\zeta=0$, *for which* p_f *denotes the left intercept of* Σ *with the outermost unstable limit cycle, if exists, there exists a singular homoclinic orbit to either the saddle-focus equilibrium* p_f *or to the outermost limit cycle on* $\{f=0,\overline{x}\leqslant x\leqslant 1\}$.

In fact, part of the condition (3.1) that $z_{\rm spk}<\overline{z}$ is more than necessary for the existence of Γ_0. It only requires $\underline{z}<z_s<\overline{z}$.

VI. RETURN MAPS AND CHAOS

The existence of a singular homoclinic orbit Γ_0 to the unstable spiral equilibrium point p_f guarantees chaotic dynamics. This can be explained in two ways.

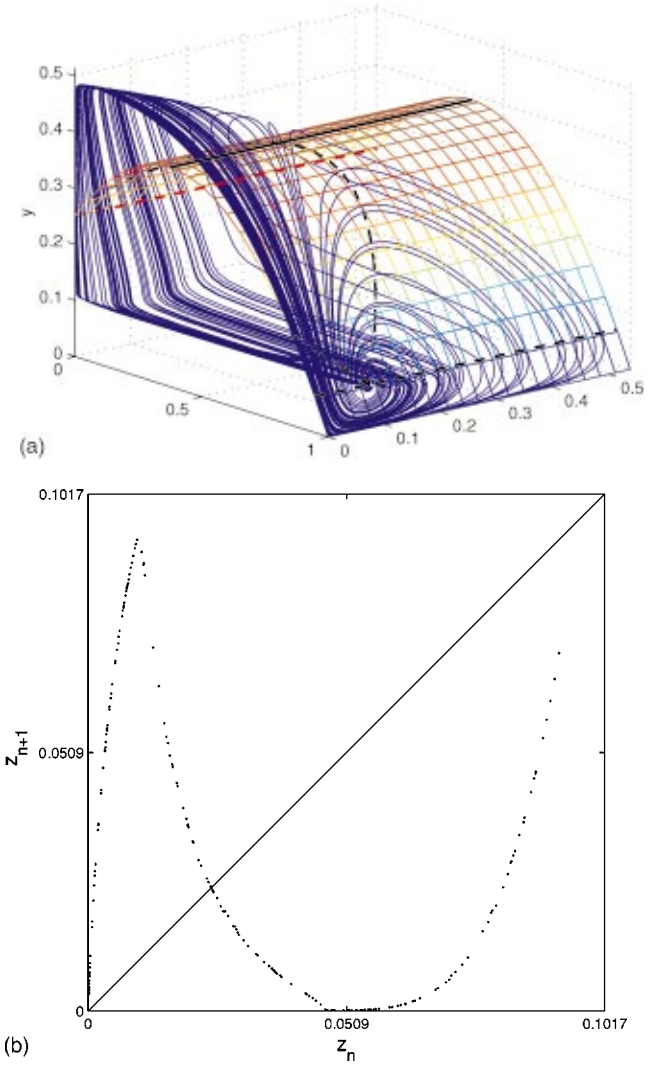

FIG. 5. (Color) Numerical simulation. (a) A perturbed attractor. (b) A Poincaré return map. Parameter values are $\zeta=0.05, \varepsilon=1, \beta_1=0.25, \beta_2=0.1, \delta_1=0.2, \delta_2=0.39$

The first follows a well-known theorem of Shilnikov from Ref. 19 which states that if there is a homoclinic orbit to a saddle-focus equilibrium point having eigenvalues $\lambda_{1,2}, \lambda_3$ satisfying $\lambda_{1,2}=\alpha\pm i\beta$ and $\lambda_3<-\alpha<0$, then in a neighborhood of the orbit there exists a chaotic orbit (see also Ref. 27). In our situation, the singular orbit Γ_0 should persist as Γ_ζ for small $0<\zeta\ll 1$ by the theory of geometric singular perturbation.[22,31,32,23] The third eigenvalue λ_3 is negative corresponding to the fast x dynamics, satisfying $\lambda_3=-O(1/\zeta)<-\alpha=-a/2$ with a as in Eq. (4.1). Hence Shilnikov's eigenvalue conditions are satisfied for small $0<\zeta\ll 1$. A major shortcoming of this approach is that we cannot conclude whether or not there is a chaotic attractor that contains the Shilnikov orbit.

The second approach does precisely what the first approach fails to do. It is based on the idea of Ref. 26, which takes advantage of the singular perturbation structure of the system to construct a singular Poincaré return map π. The map is used in turn to capture the chaotic attractor which contains the singular homoclinic orbit Γ_0. More precisely, let I be the segment of Σ left of the equilibrium point p_f, and identify each point in I with its z coordinate. Then $\pi(z)$ is defined as the singular flow-induced first return of the point z from I. Figure 4(a) illustrates the map π. Note that the two end points of I are fixed points of π, the homoclinic orbit Γ_0 corresponds to the critical point $c\in I$, and the point $\overline{z}$ corresponds to the other critical point $d\in I$. The map is increasing except between c and d. The resulting map is surely chaotic.

One type of bifurcations can also be captured by the return map as shown in Figs. 4(c) and 4(e). For the case shown, the z-nullcline $y=y_f$ moves up away from the Pontryagin landing curve Σ, which takes place when δ_2 increases. The critical point c encounters a junction-fold point[28,33,1] and the map becomes differentiable at c. Moreover, increasing δ_2 drives down the maximum $\pi(c)$ as the defining flow spends more time under the z-nullcline $y=y_f$, as illustrated in Figs. 4(c) and 4(e). Similar to Theorem 6.1 of Ref. 1, a reversed period-doubling cascade[34–36] takes place as y_f increases away from $y_{\rm spk}$.

Another type of bifurcation corresponds to the case when $\overline{z}$ moves below z_s, eliminating the singular homoclinic orbit Γ_0 in the process. This scenario occurs easily by increasing δ_1 because $\overline{z}=(\overline{x}/(\beta_1+\overline{x})-\delta_1)(\beta_1+\overline{y})$ with $\overline{x},\overline{y}$ independent of δ_1. A typical case with $\overline{z}<z_s$ is shown in Fig. 4(b). Chaotic dynamics is clearly evident when p_f lies on Σ [Fig. 4(b)] and it bifurcates into a stable period-1 point when p_f is sufficiently away from Σ (Figs. 4(d) and 4(f)).

Guided by the conditions of Eqs. (3.1), (3.2), and (4.2), a perturbed attractor characteristic of Shilnikov's saddle-focus homoclinic orbit was numerically found for Eq. (2.3). The attractor and its return map are shown in Fig. 5. The ε-parameter value $\varepsilon=1$ is of order $O(1)$, which guarantees the equilibrium point to be a saddle-focus point.

We omit here a similar analysis for the case when there exists an unstable limit cycle on $\{f=0, \overline{x}\leqslant x\leqslant 1\}$. In spite of our diligent searches, both theoretical and numerical, we failed to establish this alternative as a probable event.

VII. CLOSING REMARKS

We have demonstrated that the Rosenzweig–MacArthur's food chain model Eq. (2.1) can admit a singular Shilnikov's saddle-focus homoclinic orbit under the conditions that $\zeta=0, \underline{z}<z_{\rm spk}\leqslant z_f\leqslant\overline{z}$, $\varepsilon\geqslant\varepsilon_0$, and $\delta_2=y_{\rm spk}/(y_{\rm spk}+\beta_2)$. In comparison, the reversed period-doubling cascade phenomenon analyzed in Ref. 1 occurs under the same conditions except that $0<\varepsilon\ll 1$. The same period-doubling cascade phenomenon also occurs due to the same junction-fold structure. Put together, these results cover most of the parameter range in ε for chaos generation. We leave open the question of the existence of limit cycles on the parabola x-nullcline surface $\{f=0, \overline{x}\leqslant x\leqslant 1\}$ for which there is little supporting evidence. Also left open are a collection of questions pertaining to chaotic attractors in terms of, e.g., symbolic dynamics, natural measures, Lyapunov exponents, various measurements of dimensions. As to the relevance question of this result to ecological chaos in nature, we will withhold our commentary until the time when most, if not

all, and sufficiently many mechanisms for food chain model chaos have been properly categorized and analyzed.

[1] B. Deng, ''Food chain chaos due to junction-fold point,'' Chaos **11**, 514–525 (2001).
[2] A. J. Lotka, *Elements of Physical Biology* (Williams and Wilkins, Baltimore, 1925).
[3] V. Volterra, ''Fluctuations in the abundance of species, considered mathematically,'' Nature (London) **118**, 558–560 (1926).
[4] C. S. Holling, ''Some characteristics of simple types of predation and parasitism,'' Can. Entomologist **91**, 385–398 (1959).
[5] M. L. Rosenzweig and R. H. MacArthur, ''Graphical representation and stability conditions of predator-prey interactions,'' Am. Nat. **97**, 209–223 (1963).
[6] P. Waltman, *Competition Models in Population Biology* (SIAM, Philadelphia, 1983).
[7] S. Muratori and S. Rinaldi, ''Low- and high-frequency oscillations in three-dimensional food chain system,'' SIAM (Soc. Ind. Appl. Math.) J. Appl. Math. **52**, 1688–1706 (1992).
[8] H. L. Smith and P. Waltman, ''The theory of the Chemostat—Dynamics of microbial competition,'' *Cambridge Studies in Mathematical Biology* (Cambridge University Press, Cambridge, 1994).
[9] P. Hogeweg and B. Hesper, ''Interactive instruction on population interactions,'' Comput. Biol. Med. **8**, 319–327 (1978).
[10] M. E. Gilpin, ''Spiral chaos in a predator-prey model,'' Am. Nat. **113**, 306–308 (1979).
[11] A. Hastings and T. Powell, ''Chaos in a three-species food chain,'' Ecology **72**, 896–903 (1991).
[12] K. McCann and P. Yodzis, ''Bifurcation structure of a three-species food chain model,'' Theor. Popul. Biol. **48**, 93–125 (1995).
[13] R. K. Upadhyay and V. Rai, ''Why chaos is rarely observed in natural populations,'' Chaos, Solitons Fractals **8**, 1933–1939 (1997).
[14] B. Blasius, A. Huppert, and L. Stone, ''Complex dynamics and phase synchronization in spatially extended ecological systems,'' Nature (London) **399**, 354–359 (1999).
[15] Y. Kuznetsov, O. De Feo, and S. Rinaldi, ''Belyakov homoclinic bifurcations in a tritrophic food chain model,'' SIAM (Soc. Ind. Appl. Math.) J. Appl. Math. **62**, 462–487 (2001).
[16] D. V. Vayenas and S. Pavlou, ''Chaotic dynamics of a microbial system of coupled food chains,'' Ecol. Modell. **136**, 285–295 (2001).
[17] O. E. Rössler, ''Chaotic behavior in simple reaction systems,'' Z. Naturforsch. A **31**, 259–264 (1976).
[18] W. M. Schaffer, ''Stretching and folding in lynx fur returns: evidence for a strange attractor in nature,'' Am. Nat. **124**, 798–820 (1984).
[19] L. P. Sil'nikov, ''A case of the existence of a denumerable set of periodic motions,'' Sov. Math. Dokl. **6**, 163–166 (1965).
[20] W. A. Calder III, ''An allometric approach to population cycles of mammals,'' J. Theor. Biol. **100**, 275–282 (1983).
[21] W. A. Calder III, ''Ecological scaling: Mammals and birds,'' Annu. Rev. Ecol. Syst. **14**, 213–230 (1983).
[22] L. C. Pontryagin, ''Asymptotic behavior of solutions of systems of differential equations with a small parameter at higher derivatives,'' Izv. Akad. Nauk. SSSR Ser. Math. **21**, 605–626 (1957) (in Russian).
[23] E. F. Mishchenko, Yu. S. Kolesov, A. Yu. Kolesov, and N. Kh. Rozov, *Asymptotic Methods in Singularly Perturbed Systems*, Monographs in Contemporary Mathematics (Consultants Bureau, New York, 1994).
[24] S. Rinaldi and S. Muratori, ''Slow-fast limit cycles in predator-prey models,'' Ecol. Modell. **61**, 287–308 (1992).
[25] S. Schecter, ''Persistent unstable equilibria and closed orbits of a singularly perturbed equation,'' J. Diff. Eqns. **60**, 131–141 (1985).
[26] K. Taylor and B. Deng, ''Chaotic attractors in one-dimension generated by a singular Shilnikov orbit,'' Int. J. Bifurcation Chaos Appl. Sci. Eng. **12**, 3059–3083 (2001).
[27] B. Deng, ''On Šil'nikov's homoclinic-saddle-focus theorem,'' J. Diff. Eqns. **102**, 305–329 (1993).
[28] B. Deng, ''Constructing homoclinic orbits and chaotic attractors,'' Int. J. Bifurcation Chaos Appl. Sci. Eng. **4**, 823–841 (1991).
[29] O. De Feo and S. Rinaldi, ''Singular homoclinic bifurcations in tritrophic food chains,'' Math. Biosci. **148**, 7–20 (1998).
[30] L. P. Šil'nikov, ''On a Poincaré–Birkhoff problem,'' Math. USSR-Sbornik **3**, 353–371 (1967).
[31] N. Fenichel, ''Geometric singular perturbation theory for ordinary differential equations,'' J. Diff. Eqns. **73**, 513–527 (1979).
[32] C. Bonet, ''Singular perturbation of relaxed periodic orbits,'' J. Diff. Eqns. **66**, 301–339 (1987).
[33] B. Deng, *Folding at the genesis of chaos*, Proceedings of the First World Congress of Nonlinear Analysts (W de Gruyter, Berlin, 1996), Vol. IV, pp. 3765–3777.
[34] M. Feigenbaum, ''Quantitative universality for a class of nonlinear transformations,'' J. Stat. Phys. **19**, 25–52 (1979).
[35] P. Collet and J.-P. Eckmann, *Iterated Maps of Interval as Dynamical Systems* (Birkhauser, Boston, 1980).
[36] B. Deng, ''Glucose-induced period-doubling cascade in the electrical activity of pancreatic β-cells,'' J. Math. Biol. **38**, 21–78 (1999).